An Investigation of Hot Cracking in 5083-O Aluminum Alloy Weldments

Lot-to-lot variations in composition and orientation of the weld with respect to the rolling direction significantly affect the hot-cracking sensitivity of 5083-O aluminum plate

BY J.C. LIPPOLD, E. F. NIPPES AND W. F. SAVAGE

ABSTRACT. The hot cracking susceptibility of two lots of 5083-O aluminum plate was investigated with the aid of the Varestraint Test. Alloy 5083-O was found to be less crack sensitive than both 2014-T6 and 7039-T6 and was comparable to 6061-T6. Hot cracks were observed to initiate and propagate along grain boundaries in both the fusion zone and weld heat-affected zone.

Significant variation between the cracking sensitivity of the two lots of 5083-O was found and was related to the difference in Mg content of the lots. In addition, the effect of the orientation of the weld with respect to the rolling direction of the plate was investigated. Welds made parallel to the rolling direction were less crack sensitive than those made transverse to the rolling direction. It was found that the greater number of HAZ grain boundaries per unit length of fusion line in welds made transverse to the rolling direction was responsible for this increased cracking sensitivity.

Microsegregation of Mg during the welding operation results in the formation of a low melting eutectic liquid during the final stages of solidification. This eutectic material was observed along grain boundaries in both the fusion zone and HAZ. These grain boundaries provide a microstructure susceptible to hot cracking upon the application of sufficient augmented strain.

Introduction

The thermal expansion coefficient of aluminum alloys is roughly twice that of iron base alloys and, therefore, for the same change in temperature the shrinkage strains in aluminum weldments are roughly twice those in steel weldments. In addition, aluminum alloys exhibit a wide melting temperature range and are thus inherently sensitive to hot cracking.

Table 1—Composition of Aluminum 5083-O, Wt. %, Lot A and Lot B (Aluminum Company of America)

Element	Lot A	Lot B
Silicon	0.08	0.12
Iron	0.22	0.24
Copper	0.04	0.06
Manganese	0.64	0.60
Magnesium	4.28	4.78
Chromium	0.09	0.10
Nickel	0.00	0.00
Zinc	0.04	0.03
Titanium	0.04	0.04
Beryllium	0.000	0.000

In general, hot cracks are caused by the combination of two factors: (1) mechanically and/or thermally induced strain; and (2) a crack-susceptible microstructure. Since thermally induced strains are inherent in the process of melting and solidification, the only viable method of preventing hot cracking lies in the elimination or control of the crack-susceptible microstructure. Welding parameters, rates of solidification, alloy composition, and microsegregation are all factors which play an important role in the control of hot cracking associated with welding.

The 5000 series of aluminum alloys offers an excellent combination of corrosion resistance, strength, toughness, and weldability.[1] As a result, alloys in this series are employed in a wide variety of welded structures. Weldments in the 5083-O alloy show excellent mechanical properties at cryogenic temperatures, and unlike steels, exhibit no ductile-to-brittle transition temperature. In fact, elongation and fracture toughness of 5083-O actually improve as the temperature is decreased.

Consequently, 5083-O has been used widely for cryogenic storage tanks, in particular for the storage of liquified natural gas (LNG). Such tanks are welded using both GTAW and GMAW in all positions, often in the field. Typical welding problems include porosity, of both gas and shrinkage type, incomplete fusion, distortion, and hot cracking. In most cases these problems can be eliminated by appropriate choice of welding procedures. However, hot cracking problems are sometimes remarkably persistent and are not readily eliminated by simple changes in welding procedure.

Three types of hot cracking in LNG tanks constructed of 5083-O have been identified:[2] (1) aggravated hot-short cracking, (2) cracking of pre-

Paper presented at the 57th AWS Annual Meeting held in St. Louis, Missouri, during May 10-14, 1976.

J. C. LIPPOLD is a Graduate Assistant; E. F. NIPPES is Professor of Metallurgy and W. F. SAVAGE is Professor of Metallurgy and Director of Welding Research, Materials Engineering Department, Rensselaer Polytechnic Institute, Troy, New York.

viously deposited welds, and (3) weld shrinkage cracking (shrinkage porosity).

To some extent, these problems may be remedied by changing the welding procedure. However, such problems are not likely to be eliminated until the metallurgical factors involved are understood.

Materials and Procedure

The hot cracking sensitivity of two lots of 2 in. (5.08 cm) 5083-O aluminum plate was investigated with the aid of the Varestraint Test.[3] The remelt analyses of these lots are summarized in Table 1. Specimens were machined to dimensions of ½ × 2 × 12 in. (1.27 × 5.08 × 30.5 cm), where the ½ in. (1.27 cm) dimension represents the thickness of the specimen and the 2 in. (5.08 cm) dimension corresponds to the thickness of the original plate. All specimens tested from Lot A material were cut with the 12 in. (30.5 cm) dimension normal to the rolling direction. Two sets of specimens were machined from Lot B, one with the 12 in. (30.5 cm) dimension parallel, and the other normal to the rolling direction. All welds were made on the 2 in. (5.08 cm) wide surface parallel to the 12 in. (30.5 cm) dimension.

Specimens from both lots were tested at augmented strains ranging from ¼% to 4%, using the welding parameters listed in Table 2. Following testing, measurements of total crack length were made using a binocular microscope at 70× magnification.

Additional Varestraint specimens were prepared to determine the crack sensitivity of an all-weld-metal sample. Three autogenous GTA welds were placed on the surface of specimens from Lot A. The specimens were not constrained during the welding and care was taken to insure that the welds overlapped. The top surface of the welded specimen was then milled flat. The final thickness dimension of all specimens was 0.49 ± 0.005 in. (12.45 ± 0.13 mm). These specimens were then Varestraint tested using augmented strains ranging from ¼% to 2% and the welding parameters listed in Table 2.

Electron beam microanalysis of selected areas from two Lot-A specimens tested at 4% restraint was performed at the Alcoa Technical Center, Alcoa Center, Pa. A point-count technique was used, with an excited spot diameter not in excess of 3 μm.

Determination of the Temperature Gradient in the Base Metal Adjacent to the Fusion Zone

Two Varestraint test bars were instrumented with 0.01 in. (0.25 mm) diameter asbestos-glass-insulated, chromel-alumel thermocouples in order to determine the temperature gradient in the base metal near the fusion zone. The welding parameters used are listed in Table 2.

The emf outputs of the thermocouples were recorded during the welding operation using a multiple-channel, direct-developing, recording oscillograph. This provided a permanent record from which accurate temperature measurements could be obtained later. In order to determine the exact position of each thermocouple in the base material the surface of the welded specimen was milled away until the thermocouple weld was revealed. The test bar was then etched to reveal the fusion line and the distance from the thermocouple weld to the fusion line was measured. The logarithm of peak temperature was then plotted as a function of the distance from the fusion line.

Investigation of Crack Paths

One specimen from Lot A, tested at 4% restraint, was prepared as follows in order to investigate the 3-dimensional cracking pattern of a typical Varestraint specimen. After testing, a ½ × ¾ in. (1.27 × 1.9 cm) portion of the specimen was removed which contained the hot cracks. This sample was mounted in epoxy such that the as-welded surface with the exposed hot cracks was completely submerged in epoxy. The mounted specimen was then subjected to a high vacuum in order to force penetration of the epoxy into the cracks. After the epoxy had cured, the aluminum was dissolved away in concentrated HCl. In this fashion, an epoxy replica of the crack network was obtained. After coating with gold, macrographs were taken of the replicas with a scanning electron microscope.

Gleeble Testing

Samples machined from Lot A material were tested using the high speed time-temperature control device known as the Gleeble.[4]

Initial tests were run on the Gleeble to determine the solidus temperature. Subsequent tests were run to simulate the thermal cycles present in the HAZ and near the fusion line during welding.

Results and Discussion

The two lots of 5083-O, designated as A and B, were tested under identical conditions to determine their relative weldability. In general, all specimens exhibited similar cracking morphology. Fusion zone hot cracks appeared in a roughly semicircular array outlining the location at the trailing edge of the weld pool at the instant the augmented strain was applied. Closer examination after macroetching with Tucker's reagent revealed that all fusion zone cracks were located in the boundaries between individual grains. It has been noted previously[5,6] that during solidification the grains at the solid-liquid interface tend to grow in the direction of the maximum temperature gradient. Thus, cracks propagating in these grain boundaries are oriented roughly perpendicular to the trailing edge of the weld pool. Figure 1 is a macrograph of a Varestraint specimen tested at 4% restraint and illustrates the typical hot cracking morphology.

Comparison of Lots A and B

The relative hot cracking sensitivity of lots A and B is shown in Fig. 2 for welds transverse to the rolling direction. For augmented strains less than

Table 2—Summary of the Welding Conditions Used in Varestraint Testing of Lot-A and Lot-B, 1/2 in. (12.7 mm) Specimens

Electrode material	W-2% ThO_2, centerless ground, ⅛ in. (3.2 mm) diameter
Electrode geometry	Conical Tip, ground to 90 deg incl. angle
Electrode extension	1.5 in. (37.5 mm) from the water-cooled collet
Electrode-work distance	3/32 in. (2.4 mm), measured cold
Welding current	175 ± 10 A, DCSP
Welding voltage	15 ± 0.5 V
Travel speed	8 ipm (20.3 cm/s)
Shielding gas	Helium
Gas flow rate	70 cfh (33 liters/min)

Fig. 1—Top surface of a Varestraint specimen tested at 4% restraint. Tucker's reagent; ×6 (reduced 50% upon reproduction)

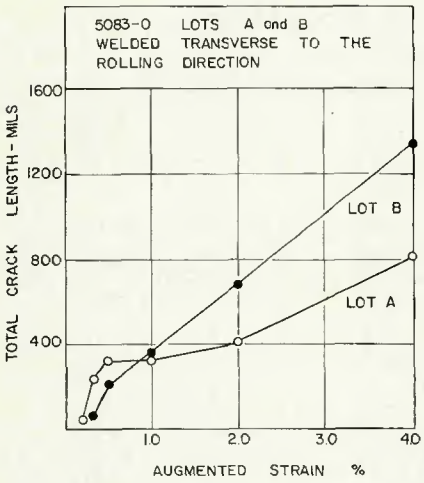

Fig. 2—Total crack length vs. percent augmented strain

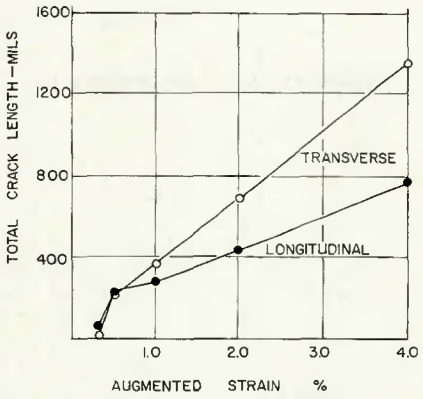

Fig. 3—Total crack length vs. percent augmented strain; lot B welded both transverse and longitudinal to the rolling direction; welded under identical conditions

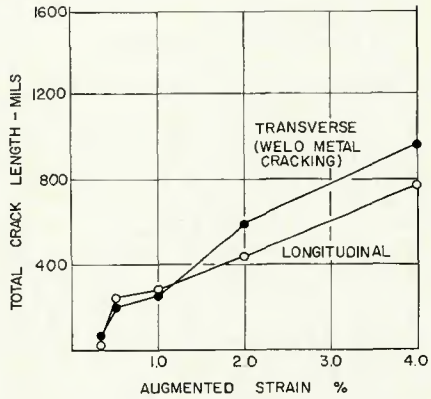

Fig. 4—Total crack length vs. percent augmented strain; lot B welded both transverse and longitudinal to the rolling direction; fusion zone cracking only

1% lot A shows a greater total crack length than does lot B. However, for augmented strains of 1% and more, lot B shows the greater total crack length. In fact, at 4% augmented strain lot B exhibits nearly 75% more cracking than lot A. Such differences in cracking sensitivity among lots of the same alloy are not uncommon, but the metallurgical factors responsible are not easy to identify. Table 1 reveals that lot A and lot B are of nearly identical composition except that lot B contains 0.50 wt. % more Mg than lot A. It seems likely, therefore, that increasing the Mg content increases the hot cracking susceptibility of 5083-O under conditions simulating a high degree of restraint.

Comparison of Welds Made Transverse and Parallel to the Rolling Direction

Sets of specimens from lot B oriented both parallel to and normal to the rolling direction also exhibited a marked difference in hot cracking susceptibility. As is shown in Fig. 3, specimens welded transverse to the rolling direction exhibit a greater total crack length than specimens welded parallel to the rolling direction at strains above ½%. At 4% augmented strain, the transverse specimen exhibited 70% more total cracking than the corresponding longitudinal specimen.

Examination of the hot cracking in the transverse and longitudinal specimens revealed that substantial HAZ cracking occurred in the transverse specimens at augmented strains above ½%, while there was essentially no HAZ cracking in the longitudinally oriented test specimens. Figure 4 compares only the fusion zone cracking for both orientations from lot B. On this basis the total cracking at all levels of restraint are more nearly comparable. Thus it may be assumed that the observed variation in overall cracking may be related to the microstructure and properties of the HAZ and base metal adjacent to the fusion zone.

The photomicrographs in Fig. 5, taken at ×70 after electropolishing, show the microstructure near the fusion boundary on the top surface of the autogenous welds made in the longitudinal and transverse orientation, respectively. The fusion zone extends upward from the reference marks AA in each case, and the microstructure of the fusion zone is essentially independent of the weld orientation except for a narrow band near the fusion line. A region of partial melting is evident in each case just below AA. Within this region the grains exhibit a characteristic substructure which becomes progressively less pronounced as the distance from the fusion line increases. This substructure is no longer detectable at a distance of 0.005 in. (0.13 mm) from the fusion line (about ⅜ in. (9.5 mm) at ×70). Note that within this region the grains in the longitudinal specimen (Fig. 5a) retain their severely elongated morphology and thus only a few grain boundaries intersect the fusion line.

On the other hand, in the weld oriented transverse to the rolling direction (Fig. 5b), the elongated grains visible in the unaffected base metal near the bottom of the micrograph appear to have been replaced by a network of more nearly equiaxed grains within the partially melted region. Consequently, many more grain boundaries intersect a unit length of fusion line in the transverse weld than in the longitudinal weld.

Thus, a crack initiated in the fusion zone and propagating radially outward from the weld pool would tend to be arrested at the edge of the fusion zone in the longitudinal weld. This crack-arresting mechanism operates because the grain boundaries, which serve as crack paths in the fusion zone, are only rarely continuous across the fusion line into the base metal. In the transverse weld specimen, on the other hand, many more grain boundaries are

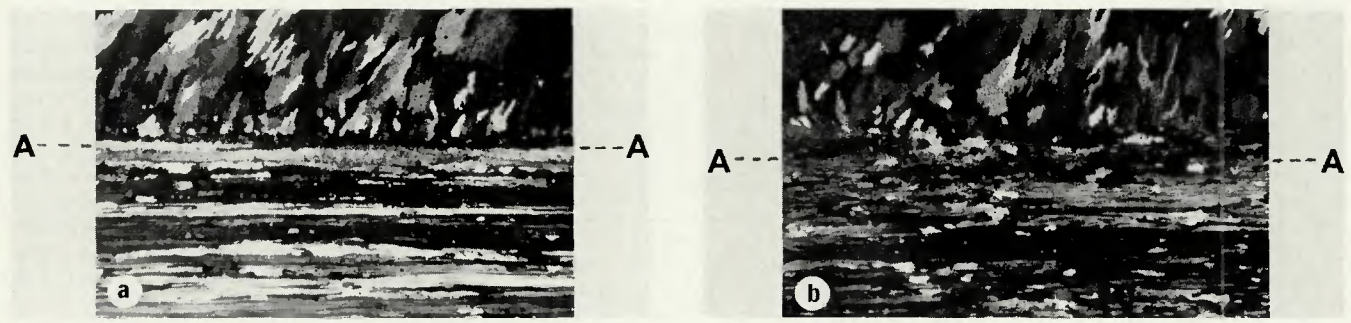

Fig. 5—Grain structure near the fusion line of welded lot B specimens: (a)—welded parallel to the rolling direction; (b)—welded transverse to the rolling direction; electropolish, polarized light, ×70 (reduced 44% upon reproduction)

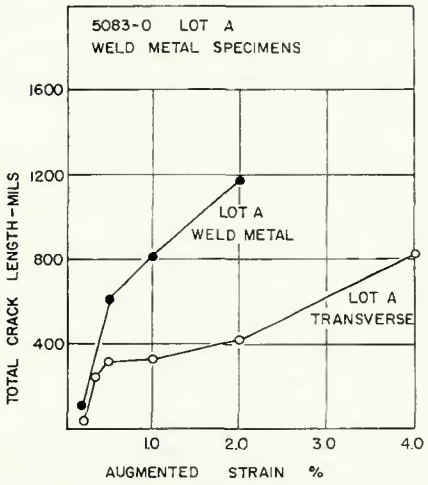

Fig. 6—Total crack length vs. percent augmented strain, lot A specimens welded transverse to the rolling direction compared to all-weld-metal lot A specimens welded under identical conditions

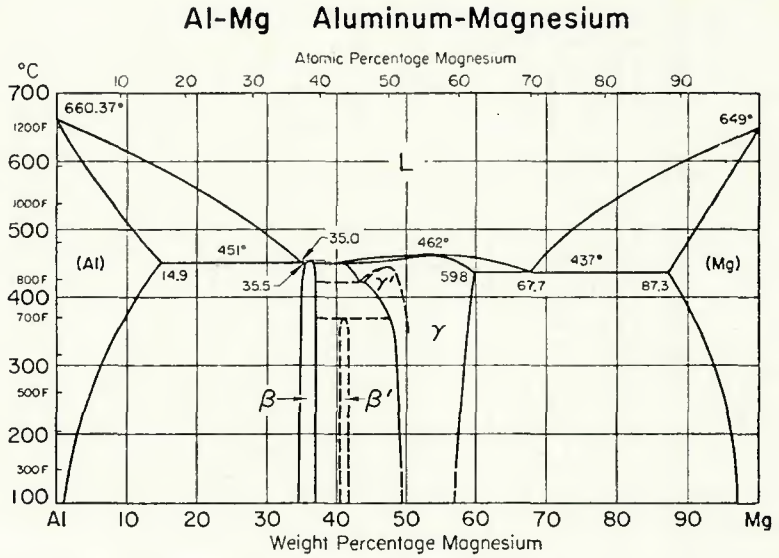

Fig. 7—Al-Mg phase diagram

continuous across a unit length of the fusion line and thus a crack which originates in the weld has a higher probability of propagating into the partially melted zone. This explains why the transverse welds experienced more cracking in the Varestraint tests.

Comparison of As-Received with All-Weld-Metal Specimens

All-weld-metal specimens produced from lot A material were tested under the same conditions as the as-received specimens from lot A in order to demonstrate the effect of grain boundary orientation on the crack-arresting tendency of the base metal. It is clearly evident from Fig. 6 that all-weld-metal specimens are more crack sensitive than lot A as-received specimens tested with a single-pass transverse weld.

Cracks were observed to propagate across the fusion line into the weld metal pad which served as the base metal. The fine grained structure of this pad provided a greater number of grain boundaries for crack initiation than were found in the as-received base metal of the lot A specimens.

Comparison of 5083-O with Other Aluminum Alloys

A final set of Varestraint tests was performed in order to compare the behavior of 5083-O with that of three other aluminum alloys tested previously in this laboratory.[7] At augmented strains above 0.25%, 5083-O was roughly comparable to 6061-T6 in resistance to hot cracking. Both 5083-O and 6061-T6 were considerably more resistant to hot cracking than 2014-T6, which in turn was slightly more resistant to hot cracking than 7039-T6.

Investigation of the Hot-Cracking Mechanisms

From the results of Varestraint tests of the two lots of 5083-O, it appears that increasing the Mg content increased the hot cracking tendency of the alloy. In addition, it was observed that all hot cracks propagated along grain boundary paths in both the fusion zone and weld heat-affected zone. In general, two types of hot cracks can be characterized by their location in the Varestraint test specimen:

1. Fusion zone hot cracks, which are associated with microsegregation produced at grain boundaries during the rapid solidification of the weld;

2. Heat-affected zone hot cracks, which are associated with microsegregation produced at grain boundaries either during the original casting and processing of the material or as a result of partial melting which occurs in the base metal next to the fusion zone during welding.

The following sections will discuss these two types of hot cracks in detail.

Microsegregation in the Fusion Zone. Rapid solidification, in both castings and fusion welds, gives rise to microsegregation of certain alloying elements. The degree of microsegregation is controlled primarily by the distribution coefficient, k*, of the alloying element involved. In general, the more the value of k departs from 1.0 the greater will be the severity of the microsegregation, all else being equal. The k value for Mg in a binary aluminum alloy is approximately 0.25 at temperatures near the solidus for C_o = 4.28 wt. % Mg.[8] During solidification of the alloy, Mg is rejected to the surrounding liquid and thus the final solid formed will be enriched in Mg. This segregation in turn lowers the effective melting temperature of the grain and cell boundary areas where the last remaining liquid transforms to solid.

Examination of the microstructure in the fusion zone indicated that a cellular growth mode occurred in areas adjacent to the fusion line. Such a growth mode results from the steep temperature gradients which are present at the fusion line. As growth continues away from the fusion line, i.e., as the temperature gradient decreases, the growth mode changes to cellular-dendritic. In both cases microsegregation is inherent in the growth process. Thus, in the case of 5083-O a high degree of Mg enrichment would be expected in the fusion zone boundary regions.

Formation of Eutectic Solid. The rejection of Mg into the liquid during dendritic solidification produces a microstructure which is potentially susceptible to hot cracking. Increased solute concentration in boundary regions, where final solidification occurs, lowers the effective solidus temperature there. These high solute boundaries are the regions in which hot cracks initiate and propagate. In addition, the increased Mg content in these boundaries promotes the formation of a low melting eutectic solid. This eutectic material was observed in backfilled cracks in both the fusion zone and weld heat-affected zone. Electron beam microprobe analysis of this material revealed that its composi-

**The equilibrium distribution coefficient, k, is defined by the ratio of C_s/C_l, where C_s and C_l are, respectively, the concentrations of solute in the solid and liquid phases in equilibrium with one another at constant temperature.*

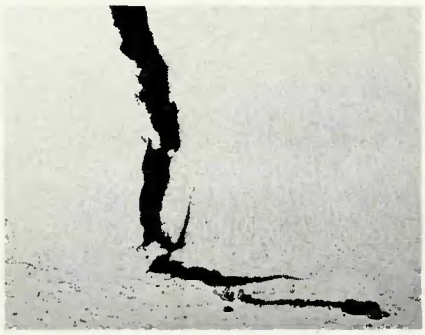

Fig. 8—Typical fusion zone hot crack, lot A specimen tested at 2% restraint; Keller's reagent; ×50 (reduced 50% upon reproduction)

tion was close to that of β (Al, Mg).

Inspection of the binary Al-Mg phase diagram in Fig. 7[9] reveals that at 844 F (451 C) a eutectic reaction between α and β occurs at 35.0 wt. % Mg. At this temperature the α phase has a composition of 14.9 wt. % Mg and β a composition of 35.5 wt. % Mg. Thus, the eutectic solid would appear to be nearly 100% β.

Since the effective solidus of the base metal, as determined from Gleeble tests, is approximately 1100 F (593 C), a wide range exists between the solidification temperature of the bulk solid and that of the eutectic material. It is within this temperature range that hot cracks are initiated and propagated.

Using a local solute-redistribution equation, the amount of liquid of eutectic composition during the final stages of solidification can be calculated. Such an equation[10] is:

$$C_s^* = kC_o \left[\frac{a}{k-1} + \left(1 - \frac{ak}{k-1}\right)\left(1 - f_s\right)^{k-1} \right]$$

where C_s^* is the solid composition at the liquid-solid interface at the instant a given fraction solid, f_s, has formed. C_o is the nominal composition of the alloy, k is the equilibrium distribution coefficient, and a is a constant dependent on the alloy system and welding parameters.

In the case of dendritic solidification, the parameter a is negligible and the equation above reduces to:[11]

$$C_s^* = kC_o (1-f_s)^{k-1}$$

At the eutectic temperature, values of C_s^* and k may be calculated from the Al-Mg phase diagram. Since the Mg composition of each lot is known (Table 1), the fraction of eutectic liquid ($1-f_s$) present during the final stages of solidification may be calculated for both lots.

Although the amount of eutectic formed was small for each lot (2-3%), lot B, due to its higher Mg content, formed nearly 20% more eutectic than lot A. This increase in eutectic liquid probably accounts for the greater hot cracking sensitivity of lot B Varestraint specimens.

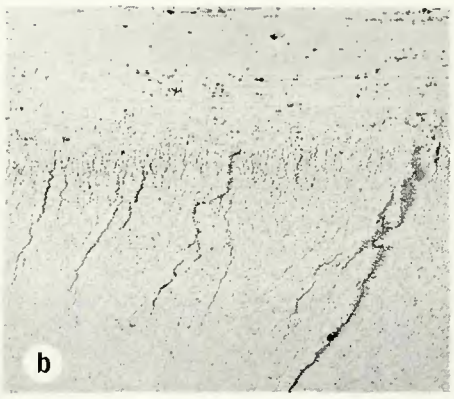

Fig. 9—Completely backfilled fusion zone hot cracks; (a)—lot A specimen, (b)—lot B specimen tested at 4% restraint; Keller's reagent; ×75 (reduced 36% upon reproduction)

Characterization of Fusion Zone Hot Cracks. Three types of fusion zone hot cracks were observed in this investigation:

1. Open cracks, generally macroscopic in nature, which exhibited little or no backfilling;
2. Partially backfilled cracks of moderate size which exhibited various degrees of backfilling;
3. Completely backfilled cracks, which were generally the smallest cracks observed.

The crack in Fig. 8 would be termed an "open" crack since there is little or no evidence of backfilling by the eutectic material. The crack was initiated near the top of the photomicrograph, at the trailing edge of the weld pool, and propagated radially outward. It may be observed that the crack propagates parallel to solidification substructure present in the fusion zone. Upon reaching the fusion line, an abrupt change in crack direction occurs due to the grain orientation of the base metal.

Fig. 10—Backfilled fusion zone hot crack propagating along a grain boundary, lot A specimen; Keller's reagent; ×250 (reduced 50% upon reproduction)

Some degree of backfilling, or crack "healing"[12] of fusion zone cracks was observed in both lots of 5083-O. Figure 9 (a and b) represent completely backfilled cracks produced by a 4% augmented strain in Lot A and B specimens, respectively. The specimen in Fig. 9a was welded transverse to the rolling direction, whereas the specimen in Fig. 9b was welded parallel to the rolling direction. The backfilled material of eutectic composition is readily identified as a darker etching material outlined by grain and cell boundaries in the fusion zone.

Mechanism of Crack Formation. A section of a completely backfilled hot crack located near the fusion line is shown at 250× in Fig. 10. Isolated pockets of eutectic material can be observed along a fusion zone grain boundary. Upon application of sufficient augmented strain, the solid bridges which separate these eutectic pockets rupture, allowing the low melting liquid to be drawn into the resulting crack by capillary action. If the strain is sufficiently large, the capillary forces are insufficient to draw the low melting liquid into the crack, and an open crack, such as that shown in Fig. 8, results.

Heat-Affected Zone Hot Cracking

Concurrent with the effects of solidification in the fusion zone, considerable metallurgical change occurs in the surrounding base metal. Within a narrow region of the base metal adjacent to the fusion line, rapid thermal cycles with peak temperatures up to the effective solidus temperature are experienced. This region is generally referred to as the weld heat-affected zone (HAZ). It is within this zone that numerous hot cracks were observed in both lots of 5083-O.

Characteristics of HAZ Hot Cracks. In both lots of material, the hot cracks observed in the HAZ were completely, or nearly completely, backfilled with low melting, solute-rich liquid. In most cases complete backfilling is possible due to the small size and shallow depth of the cracks. Several HAZ cracks which were observed during the tabulation of crack length data disappeared upon further polishing. Most HAZ hot cracks were observed to extend less than 0.025 in. (0.64 mm) below the as-welded surface. As the HAZ crack propagates into the test specimen normal to the welded surface, its distance from the fusion line increases as a result of the concavity of the weld pool. Thus, as the crack extends into the specimen, the effective solidus of the low melting phase at the grain boundaries is encountered and further propagation of the crack becomes much more difficult.

As observed in the study of fusion zone hot cracks, crack propagation in the HAZ occurs exclusively along grain boundary paths. Crack morphologies in specimens welded transverse to the rolling direction would be expected to be more irregular than crack morphologies in the longitudinal specimens as a result of the less elongated grain structure in the base metal. Figure 11 is a panorama of such an irregular cracking pattern at 150×. The backfilled crack closest to the fusion line runs parallel to the fusion line along a HAZ grain boundary. Upon reaching the end of this grain, crack propagation occurs both parallel and perpendicular to the fusion line along grain boundary paths, giving rise to an irregular crack morphology surrounding the HAZ grain. Thus, this backfilled crack roughly outlines a grain in the HAZ. Similar crack patterns may be observed in Fig. 9b.

In specimens welded parallel to the rolling direction the irregular pattern observed in Fig. 11 was not in evidence. Cracks were observed to run parallel to the fusion line, and only occasionally did they extend into the HAZ. The small number of favorably oriented grain boundaries in the HAZ made crack propagation into the HAZ unlikely.

Temperature Gradient in the HAZ Adjacent to the Fusion Line. With the aid of the experimentally determined temperature gradient in the base metal adjacent to the fusion zone, the temperature range in which HAZ hot cracks initiate and propagate can be estimated.

Hot cracks observed in Fig. 11 extended into the HAZ a distance of approximately 0.020 in. (0.51 mm). Reference to the measured temperature gradient in the region adjacent to the fusion line indicates that much of this region in which cracks formed and propagated experiences peak temperatures in excess of the effective solidus of the bulk solid (determined by Gleeble tests to be about 1100 F (593 C)). Thus, it appears that HAZ crack initiation occurs in the partially melted zone. In this zone, temperatures are sufficiently high to produce melting along grain boundaries. During resolidification in this partially melted region microsegregation of Mg occurs which permits formation of the eutectic liquid. Upon application of the strain during the Varestraint test such boundary areas are thus susceptible to hot crack formation.

Fig. 11—Panorama illustrating the transition from the base metal to the HAZ to the fusion zone in a lot B specimen, welded transverse to the rolling direction; Keller's reagent; ×150 (reduced 50% upon reproduction)

Fig. 12—Liquation of grain boundary regions in the HAZ; electropolish, ×750 (reduced 50% upon reproduction)

HAZ Hot Cracking Mechanism. Cracks initiated in the partially melted zone were observed to extend away from the fusion line into the HAZ along grain boundary paths. Temperatures exceeding the 1100 F (593 C) solidus temperature are experienced in the HAZ at distances up to 0.020 in. (0.51 mm) from the fusion line. Figure 12 is indicative of HAZ grain boundary appearance in regions 0.015 to 0.020 in. (0.38 to 0.51 mm) from the fusion line, within the partially melted region. Dark etching regions in the boundaries represent areas where preferential liquation has occurred at temperatures above the solidus. Under the influence of sufficient augmented strain, the "bridges" of material between these liquated regions break, and low melting liquid from the partially melted zone backfills the opened grain boundaries.

The presence of HAZ hot cracks was not observed in specimens tested at augmented strains of less than 1% in either Lot-A or Lot-B material. *The existence of a minimum value of augmented mechanical strain to cause HAZ hot cracking is thus apparent.* Evidently, augmented strains less than 1% are insufficient to rupture the weakened grain boundaries. Thus, the propagation of hot cracks initiated in the partially melted zone is not possible along HAZ grain boundaries with small values of augmented strain.

At distances greater than 0.020 in. (0.51 mm) from the fusion line the peak temperature in the base metal during welding is insufficient to produce a crack-susceptible microstructure.

Gleeble Tests. Base metal specimens of 5083-O tested in the vicinity of the solidus temperature with the aid of the Gleeble reproduced the microstructure observed in the HAZ and partially melted region of the welded Varestraint specimens.

Pockets of liquated material were observed along grain boundaries. In addition, failure of the Gleeble test specimens occurred exclusively along these semiliquid boundaries.

Thus, it is likely that microsegregation during the casting and working of the alloy produces a microstructure which is susceptible to hot cracking in the presence of a suitable thermal cycle and a critical level of augmented strain.

Subsurface Cracks

During the course of this investigation the 3-dimensional morphology of hot cracks was studied. Normally, only the length of surface cracks is considered in the Varestraint test. The transverse weld section pictured at ×4 in

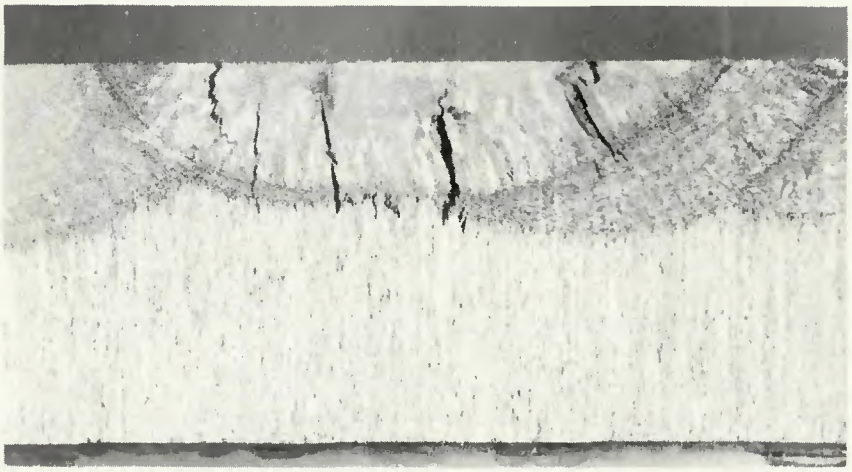

Fig. 13—Subsurface weld hot cracking in a lot A all-weld-metal test specimen, tested at 2% restraint; Tucker's reagent; ×4, not reduced

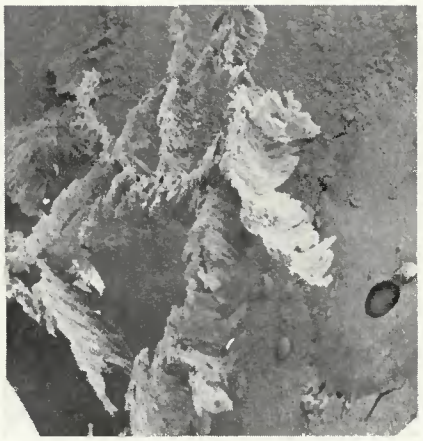

Fig. 14—Epoxy replica of sub-surface fusion zone hot cracks, scanning electron micrograph; ×20 (reduced 35% upon reproduction)

Fig. 13 is an example of the extent of subsurface cracking which occurs during a Varestraint test. The specimen was subjected to 2% strain and was taken from the group of all-weld-metal specimens whose cracking behavior was illustrated in Fig. 6 (note the prior weld passes).

In order to study the overall appearance of the crack network, some mounts containing specimens subjected to 4% strain were immersed in concentrated HCl in order to dissolve the alloy. Since, as a step in the mounting process, the specimens were subjected to a vacuum while immersed in the liquid epoxy, the cracks were backfilled with epoxy which, when cured, formed a three-dimensional replica of the cracks.

Figure 14 is a scanning electron micrograph from a replica of a lot A specimen tested at 4% restraint. Cracks can be seen to join in a complex pattern below the weld surface. The flat surface represents the surface of the weld and base metal. The cracks extend upward out of the plane of the paper.

Twinned Growth

During the examination of welded surfaces the presence of large grains growing near the weld centerline was frequently noted. Figure 1 shows several such grains which extended through the cracking region near the center of the weld. The phenomenon is referred to[6] as "feather growth" due to the feathery appearance of the grain. Figure 15 shows the appearance of these grains at 50×.

This effect has been studied to some extent in aluminum castings.[6-13] The solidification proceeds by what is known as twinned growth since the growth tends to occur parallel to the twin planes and grains consist of many parallel twins. It has been observed

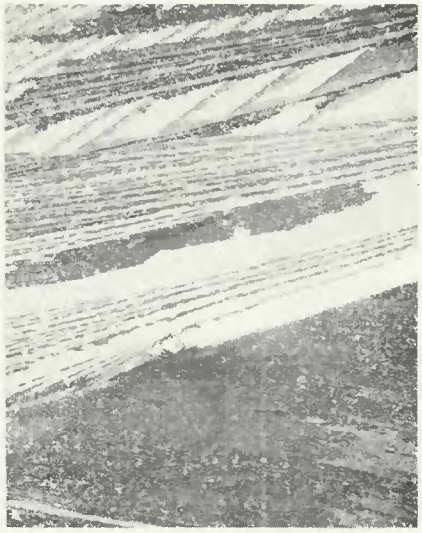

Fig. 15—Propagation of a fusion zone hot crack along the boundary of a twinned crystal; electropolish, polarized light; ×50 (reduced 35% upon reproduction)

that cooling rates such as those found in small castings and weldments, are an important factor in the occurrence of twinned growth. In the present case, the use of high energy inputs (generally greater than 20 kJ/in., 7.9 kJ/cm) and slow travel speeds promoted twinned growth in this alloy.

In all Varestraint specimens exhibiting twinned growth, no hot cracking was observed to occur within, or propagate through, such regions. In Fig. 15 a crack, which appears white, propagated along the interface between the twinned crystal and the adjacent grain. It appears that during twinned growth, solute segregation occurs only at the grain boundaries since no solidification substructure is evident. This is an important factor in preventing hot crack initiation and propagation within the so-called feather crystals.

Conclusions

Varestraint Test Results

The following conclusions pertain to the results of Varestraint tests:

1. Lot B was found to be more susceptible to hot cracking than Lot A for welds made transverse to the rolling direction.
2. It appears that the increased hot cracking susceptibility of Lot B is related to its higher Mg content.
3. Welds made transverse to the rolling direction experienced more hot cracking than welds made parallel to the rolling direction.
4. Increased total crack length of transverse welded specimens in relation to specimens welded parallel to the rolling direction was a result of greater HAZ hot cracking in the transverse welded specimens.
5. All-weld-metal Varestraint specimens exhibited a greater total crack length than as-received base metal Varestraint specimens.
6. 5083-O was comparable to 6061-T6 and superior to 2014-T6 and 7039-T6 in resistance to hot cracking.
7. Hot cracks were observed primarily along grain boundaries in both the fusion zone and HAZ.

Fusion-Zone Hot Cracking

The following conclusions pertain to the results of metallographic investigation of fusion-zone hot cracking:

1. During weld solidification, the microsegregation of Mg results in the formation of a low melting eutectic material which was observed to backfill into small fusion-zone cracks.
2. Fusion-zone hot cracks propagate when sufficient augmented strain ruptures bridges of solidified material separating pockets of eutectic liquid along grain boundaries.
3. Subsurface hot cracks were nu-

merous in specimens tested at high levels of augmented strain.

4. Twinned growth, commonly referred to as "feather" crystals, was observed in the fusion zone when high energy inputs and slow travel speeds were employed.

HAZ Hot Cracking

The following conclusions pertain to the results of metallographic investigation of HAZ hot cracking:

1. A partially melted zone was observed to extend approximately 0.005 in. (0.13 mm) from the fusion line into the HAZ.

2. Increased grain boundary area per unit length of fusion line in specimens welded transverse to the rolling direction resulted in more HAZ hot cracking than in specimens welded parallel to the rolling direction.

3. Eutectic liquid completely backfilled most HAZ hot cracks.

4. A critical level of augmented strain was necessary to propagate HAZ hot cracks along semiliquid grain boundaries.

Acknowledgments

The authors are grateful to the Alcoa Foundation for financial support of the fellowship under which this investigation was conducted.

References

1. Blaze, Gary C., "The 5000-Series Alloys Suitable for Welded Structural Applications," Aluminum Company of America, New Kensington, Pa., 1972.

2. "Production Welding of Aluminum Tankage for LNG," Alcoa Process Development Laboratories, Report No. A-135.

3. Lundin, C. D., and Savage, W. F., "Application of the Varestraint Technique to the Study of Weldability," *Welding Journal*, 31(11), Nov. 1966, Res. Suppl., pp. 534-s to 545-s.

4. Nippes, E. F., and Savage, W. F., "Development of Specimen Simulating Weld Heat-Affected Zones," *Welding Journal*, 28(11), Nov. 1949, Res. Suppl., pp. 599-s to 616-s.

5. Savage, W. F., Lundin, C. D., and Aronson, A. H., "Weld Metal Solidification Mechanics," *Welding Journal*, 44(4), April 1965, Res. Suppl., pp. 175-s to 181-s.

6. Chalmers, B., *Principles of Solidification*, John Wiley and Sons, Inc., New York, 1964.

7. Lundin, C. D., and Savage, W. F., "The Evaluation of the Weldability of Structural Alloys with the Varestraint Test," Technical Report AFML-TR-68-48, 1968.

8. Willey, L. A., and Wright, E. H., "Aluminum Binary Equilibrium Diagrams," Technical Paper No. 15, Alcoa Research Laboratories, 1960.

9. *Metals Handbook*, 8th Edition, American Society for Metals, Vol. 9, p. 261.

10. Bower, T. F., Brody, H. D., Flemings, M. C., *Trans. AIME*, 236, Appendix A, 1966, p. 824.

11. Flemings, M. C., *Solidification Processing*, McGraw-Hill, Inc., New York, 1974, p. 142.

12. Borland, J. C., "Generalized Theory of Super-Solidus Cracking in Welds (and Castings)," *British Welding Journal*, 7(8), 1960.

13. Aust, K. T., Krill, F. M. and Morral, F. R., "Observations on Twinning in Semi-Continuous Cast Aluminum," *Journal of Metals*, 192, August, 1952.

AWS A2.4-76—Symbols for Welding and Nondestructive Testing

Provides the means for placing complete welding information on drawings. Symbols in this publication are intended to be used to facilitate communications among designers and shop and fabrication personnel. Many changes were made from the previous edition in recognition of the increasingly international use of welding symbols. Illustrations showing brazing and its symbols have been added to more clearly define usage.

Part B, Nondestructive Testing Symbols, establishes the symbols for use on drawings to specify nondestructive examination for determining the soundness of materials.

The price of A2.4-76 *Symbols for Welding and Nondestructive Testing* is $5.00. Discounts: 25% to A and B members; 20% to bookstores, public libraries and schools; 15% to C and D members. Send your orders to the American Welding Society, 2501 N.W. 7th St., Miami, FL 33125. Florida residents add 4% sales tax.

AWS A5.17-76—Specification for Bare Carbon Steel Electrodes and Fluxes for Submerged Arc Welding

Prescribes requirements for carbon steel electrodes and fluxes for submerged arc welding of carbon and low alloy steels

A5.17-76 covers Classification and Acceptance of Electrodes and Fluxes, Chemical Analysis of Electrodes, and Required Tests for Classifying Fluxes. Appendix A: Guide to AWS Classification of Bare Carbon Steel Electrodes and Fluxes for Submerged Arc Welding and Appendix B: Metric Equivalents have been added for your convenience.

The price of AWS A5.17-76, *Specification for Bare Carbon Steel Electrodes and Fluxes for Submerged Arc Welding* is $3.50. Discounts: 25% to A and B members; 20% to bookstores, public libraries and schools; 15% to C and D members. Send your orders to the American Welding Society, 2501 N.W. 7th St., Miami, FL 33125. Florida residents add 4% sales tax.